

## 代用電荷法による Hele-Shaw 問題の数値計算<sup>1)</sup>

### A charge simulation method for the computation of Hele-Shaw problems

東京大学大学院数理科学研究科 榊原 航也 (Koya SAKAKIBARA)  
Graduate School of Mathematical Sciences, The University of Tokyo<sup>2)</sup>

and

明治大学理工学部 矢崎 成俊 (Shigetoshi YAZAKI)  
School of Science and Technology, Meiji University<sup>3)</sup>

#### Abstracts.

The solutions to the classical Hele-Shaw problem are discretized in space by means of a modified charge simulation method (CSM) combined with the asymptotic uniform distribution method, and then a system of ordinary differential equations is obtained, which is solved by the usual fourth order Runge-Kutta method. The Hele-Shaw problem has curve-shortening (CS) and area-preserving (AP) properties. Under our scheme, the asymptotic CS-property and the AP-property are satisfied theoretically in a discrete sense, respectively, while simple boundary element method (BEM) does not satisfy these properties in general. Numerical experiments by the modified CSM and BEM will be shown.

## 1 Introduction

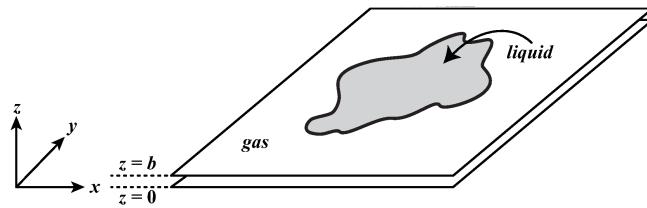
The Hele-Shaw problem is description of a motion of viscous fluid in a quasi two-dimensional space, which was starting from a short paper [4] in 1898 by Henry Selby Hele-Shaw (1854–1941). In his experiment, viscous fluid is sandwiched between two parallel plates with a narrow gap (Figure 1.1), and the apparatus is called Hele-Shaw cell. He succeeded to visualize stream lines by means of colored water in the cell. Mathematically, the Hele-Shaw problem is reduced from Navier-Stokes equations via stationary Stokes approximation, parabolic-shape approximation of the velocity profile, and assumption of the Laplace re-

---

<sup>1)</sup>Manuscript for “新時代の科学技術を牽引する数値解析学”, October 8 – 10, 2014 at RIMS, Kyoto University. This work was supported by the Program for Leading Graduate Schools, MEXT, Japan (KS) and KAKENHI No.26610031 (SY).

<sup>2)</sup>3-8-1 Komaba, Meguro-ku, Tokyo 153-8914, Japan. *E-mail:* ksakaki@ms.u-tokyo.ac.jp

<sup>3)</sup>1-1-1 Higashi-Mita, Tama-ku, Kanagawa 214-8571, Japan. *E-mail:* syazaki@meiji.ac.jp

Figure 1.1: Hele-Shaw cell with the gap  $b$ 

lation on the boundary, that is, the problem is stated as follows (see [8, 3] in detail).

$$\begin{cases} \Delta p = 0 & \text{in } \Omega(t), \\ p = \gamma k & \text{on } \mathcal{C}(t), \\ V = -\nabla p \cdot \mathbf{N} & \text{on } \mathcal{C}(t), \end{cases} \quad (1.1)$$

where  $\Omega(t) \subset \mathbb{R}^2$  is region occupied by fluid,  $\mathcal{C}(t) = \partial\Omega(t)$  is the boundary,  $p$  is the pressure function,  $k$  is the curvature (sign convention is the way that  $k = 1$  if  $\mathcal{C}(t)$  is a unit circle),  $\gamma > 0$  is the surface tension coefficient,  $\mathbf{N}$  is the unit outward normal vector, and  $V$  is the normal velocity. See Figure 1.2 (in the figure,  $\mathbf{x}$  is the position vector and  $\mathbf{T}$  is the unit tangent vector).

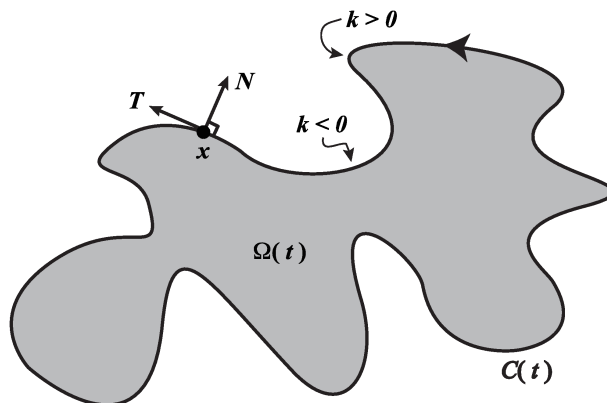


Figure 1.2: Liquid in a Hele-Shaw cell

Thus the Hele-Shaw problem is stated as a kind of moving boundary problems determining unknown function  $p$  and unknown fluid region  $\Omega$ . It can be described in another way such as follows. Let  $\mathbf{u}$  be the velocity vector of two-dimensional fluid. Then the harmonicity of the pressure  $p$  is an expression of continuation derived from the Darcy's law  $\mathbf{u} = -\nabla p$  and the incompressible condition of fluid  $\text{div } \mathbf{u} = 0$ , and the normal velocity  $V$  is derived from mass conservation law  $\partial \mathbf{x} / \partial t = \mathbf{u}$ .

The purpose of the present paper is that for (1.1) we present a simple numerical scheme by means of a modified charge simulation method combined with the asymptotic uniform distribution method.

The charge simulation method (CSM) is a numerical technique for potential problems. The idea is very simple, that is, the solution is approximated by linear combination of fundamental solutions. Then CSM is a kind of method of fundamental solutions. For instance, let us think about the Laplace problem in bounded region, say  $\mathcal{D} \subset \mathbb{R}^2$  with a smooth boundary  $\mathcal{C} = \partial\mathcal{D}$ . Under CSM, first, we take finite number (say  $n$ ) of approximate points (the collocation points) on  $\mathcal{C}$  and the same number of singular points (the charge points) in outside of  $\overline{\mathcal{D}}$ , and second, determine coefficients of linear combination of fundamental solutions equal to a given data at the collocation points. If position of the collocation points and the charge points satisfies a “nice” condition, then the approximate error has exponential decay such as  $a^{-n}$  ( $a > 1$ ) [5]. This is remarkable error estimate compared with simple the finite difference method (FDM), the finite element method (FEM) or the boundary element method (BEM) which have the error order  $n^{-a}$  ( $a > 0$ ) in general. On the other hand, unfortunately, the “nice” condition is theoretically unclear at this stage, and the condition is determined by trial and error, so far. Hence finding the condition is an open problem even for potential problems in a fixed domain. To the best of our knowledge, application of CSM for moving boundary problem is quite a few: for instance, CSM for stationary perfect fluid of rotation free in outside of a circle in the plane [14], and CSM combined with the level set method for external Hele-Shaw problem without surface tension [7].

The Hele-Shaw problem has two properties: fluid area is preserved in time and the total length of the boundary is decreasing in time. One of features of our scheme is to realize the curve-shortening property asymptotically in a discrete sense by means of the normal velocity determined by a modified invariant scheme of CSM, so-called Murota’s invariant scheme [9, 10]. Another feature is to realize the area-preserving property by means of the tangential velocity determined by a modified CSM and the asymptotic uniform distribution method (UDM) [12]. Note that under UDM, we have stable numerical computation.

Of course, there are many ways to solve the Hele-Shaw problem numerically (see selected just a few papers or a monograph [3, 13, 6, 15]). However, many of known schemes did not focus on making schemes which preserve a variational structure of the Hele-Shaw problem such as curve-shortening property and area-preserving property.

## 2 Two properties of solutions to the Hele-Shaw problem (1.1)

Let  $t \geq 0$  be the time parameter. Assume that a smooth Jordan curve  $\mathcal{C}(t) : \mathbf{x}(u, t) \in \mathbb{R}^2$ , parameterized by  $u \in [0, 1]$ , evolves according to the following evolution law of given the normal velocity  $V$  and the tangential velocity  $\alpha$  (Figure 1.2).

$$\partial_t \mathbf{x} = \alpha \mathbf{T} + V \mathbf{N}. \quad (2.1)$$

Here  $\partial_t = \partial/\partial t$  is the time derivative. It is known that, under a suitable condition, the value of  $\alpha$  does not affect the shape of the solution curve [2].

Let  $L(t)$  be the total length of  $\mathcal{C}(t)$ ,  $\Omega(t)$  the bounded region enclosed by  $\mathcal{C}(t)$ , and  $A(t)$  the area of  $\Omega(t)$ . Then the time evolution of  $L$  and  $A$  are given as follows.

$$\partial_t L(t) = \int_{\mathcal{C}(t)} kV ds, \quad \partial_t A(t) = \int_{\mathcal{C}(t)} V ds,$$

where  $s = s(u, t)$  is the arc-length parameter, and the integral means

$$\int_{\mathcal{C}(t)} \mathbf{F} ds = \int_0^1 \mathbf{F} g(u, t) du \quad (g(u, t) = |\partial_u \mathbf{x}(u, t)| \text{ is called the local length}).$$

If the pressure  $p$  and the curve  $\mathcal{C}(t)$  are the solution to the Hele-Shaw problem (1.1), then for the time evolution of  $L(t)$  we have

$$\begin{aligned} \partial_t L(t) &= \int_{\mathcal{C}(t)} kV ds = -\frac{1}{\gamma} \int_{\mathcal{C}(t)} p \nabla p \cdot \mathbf{N} ds = -\frac{1}{\gamma} \iint_{\Omega(t)} \operatorname{div}(p \nabla p) dx dy \\ &= -\frac{1}{\gamma} \iint_{\Omega(t)} (p \Delta p + |\nabla p|^2) dx dy = -\frac{1}{\gamma} \iint_{\Omega(t)} |\nabla p|^2 dx dy \leq 0. \end{aligned}$$

Hence the Hele-Shaw problem has the property of curve-shortening. We call it **CS-property**.

Also, for the time evolution of  $A(t)$  we have

$$\begin{aligned} \partial_t A(t) &= \int_{\mathcal{C}(t)} V ds = - \int_{\mathcal{C}(t)} \nabla p \cdot \mathbf{N} ds \\ &= - \iint_{\Omega(t)} \operatorname{div}(\nabla p) dx dy = - \iint_{\Omega(t)} \Delta p dx dy = 0. \end{aligned}$$

Hence the Hele-Shaw problem has the property of area-preserving. We call it **AP-property**.

### 3 Numerical scheme

The purpose of this section is to present numerical scheme by means of a modified charge simulation method combined with the asymptotic uniform distribution method, which approximates the solution  $p$  and the solution curve  $\mathcal{C}$  to Hele-Shaw problem (1.1), and satisfies asymptotic CS-property and AP-property theoretically in a discrete sense.

A smooth closed curve  $\mathcal{C}$  is discretized by a closed polygonal curve  $\Gamma$  as follows. Let  $\Gamma = \bigcup_{i=1}^n \Gamma_i$  be an  $n$ -sided closed polygonal plane curve, where

$$\Gamma_i = [\mathbf{x}_{i-1}, \mathbf{x}_i] := \{(1 - \lambda)\mathbf{x}_{i-1} + \lambda\mathbf{x}_i \mid \lambda \in [0, 1]\}$$

is the  $i$ -th edge and  $\mathbf{x}_i \in \mathbb{R}^2$  is the  $i$ -th vertex ( $i = 1, 2, \dots, n$ ;  $\mathbf{x}_0 = \mathbf{x}_n$ ,  $\mathbf{x}_{n+1} = \mathbf{x}_1$ ). See Figure 3.1.

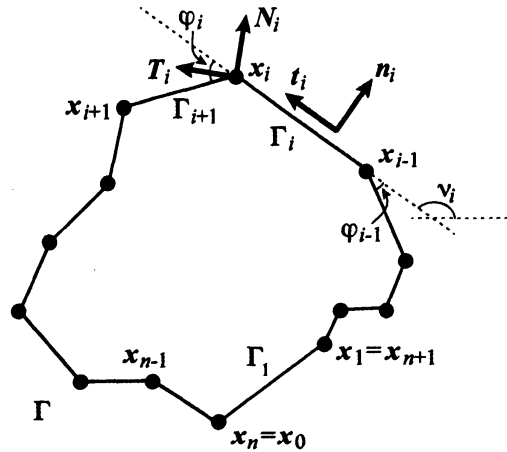


Figure 3.1: A closed polygonal curve in the plane  $\mathbb{R}^2$

Let  $\Gamma(t) = \bigcup_{i=1}^n \Gamma_i(t)$  be an  $n$ -sided closed polygonal plane curve continuously in time starting from  $\Gamma(0) = \Gamma$ , where  $\Gamma_i(t) = [\mathbf{x}_{i-1}(t), \mathbf{x}_i(t)]$  is the  $i$ -th edge, and  $\mathbf{x}_i(t) \in \mathbb{R}^2$  is the  $i$ -th vertex for  $i = 1, 2, \dots, n$  and  $t \geq 0$ . The polygonal curve  $\Gamma(t)$  moves according to the evolution law:

$$\dot{\mathbf{x}}_i = \alpha_i \mathbf{T}_i + V_i \mathbf{N}_i \quad (i = 1, 2, \dots, n), \quad (3.1)$$

where  $\dot{F} = dF/dt$  is the time derivative of  $F$ , and  $\mathbf{T}_i$  is the  $i$ -th unit tangent vector and  $\mathbf{N}_i = -\mathbf{T}_i^\perp$  is the  $i$ -th unit outward normal vector at the  $i$ -th vertex  $\mathbf{x}_i$ , which will be defined later ( $(a, b)^\perp = (-b, a)$ ). Then  $\alpha_i$ 's and  $V_i$ 's are the tangential and the normal velocities at  $\mathbf{x}_i$ , respectively. The evolution equations (3.1) correspond to a discretization of the evolution equation (2.1).

### 3.1 Algorithm

Since  $\mathbf{N}_i = -\mathbf{T}_i^\perp$  holds, the evolution equations (3.1) are rewritten as

$$\dot{\mathbf{x}}_i = \alpha_i \mathbf{T}_i - V_i \mathbf{T}_i^\perp \quad (i = 1, 2, \dots, n),$$

and by the following our scheme,  $\{\mathbf{T}_i\}_{i=1}^n$ ,  $\{V_i\}_{i=1}^n$  and  $\{\alpha_i\}_{i=1}^n$  in the right hand side can be described as a function of  $\{\mathbf{x}_i\}_{i=1}^n$ . Therefore the evolution equations can be rewritten as the following system of ordinary differential equations (ODEs):

$$\dot{\mathbf{x}}(t) = \mathbf{f}(\mathbf{x}(t)), \quad \begin{cases} \mathbf{x}(t) = (\mathbf{x}_1(t), \mathbf{x}_2(t), \dots, \mathbf{x}_n(t)) \in \mathbb{R}^{2 \times n}, \\ \mathbf{f} = (\mathbf{f}_1, \mathbf{f}_2, \dots, \mathbf{f}_n): \mathbb{R}^{2 \times n} \rightarrow \mathbb{R}^{2 \times n}; \mathbf{x} \mapsto \mathbf{f}(\mathbf{x}). \end{cases}$$

In this paper, we use the usual fourth order Runge-Kutta method for solving the above system of ODEs.

Under our scheme,  $\{\mathbf{T}_i\}_{i=1}^n$ ,  $\{V_i\}_{i=1}^n$  and  $\{\alpha_i\}_{i=1}^n$  are obtained in three steps as follows.

**Step 1:** Compute  $\{\mathbf{T}_i\}_{i=1}^n$  by  $\mathbf{T}_i = (\cos \nu_i^*, \sin \nu_i^*)^\top$  ( $i = 1, 2, \dots, n$ ) in §3.2, where  $\nu_i^* = (\nu_i + \nu_{i+1})/2$  and  $\nu_i$  is the  $i$ -th tangent angle:

$$\frac{\mathbf{x}_i - \mathbf{x}_{i-1}}{r_i} = (\cos \nu_i, \sin \nu_i)^\top, \quad r_i = |\mathbf{x}_i - \mathbf{x}_{i-1}| \quad (i = 1, 2, \dots, n).$$

**Step 2:** Compute  $\{V_i\}_{i=1}^n$  by a modified CSM in §3.4.

**Step 3:** Compute  $\{\alpha_i\}_{i=1}^n$  from  $\{r_i\}_{i=1}^n$ ,  $\{\nu_i\}_{i=1}^n$  and  $\{V_i\}_{i=1}^n$  by UDM in §3.5.

### 3.2 Step 1: Compute $\{\mathbf{T}_i\}_{i=1}^n$

The length of  $\Gamma_i$  is denoted by  $r_i = |\mathbf{x}_i - \mathbf{x}_{i-1}|$ . The  $i$ -th unit tangent vector  $\mathbf{t}_i$  can be defined as  $\mathbf{t}_i = (\mathbf{x}_i - \mathbf{x}_{i-1})/r_i$ , and the  $i$ -th unit outward normal vector  $\mathbf{n}_i = -\mathbf{t}_i^\perp$ . Then the  $i$ -th tangent angle  $\nu_i$  is obtained from  $\mathbf{t}_i = (\cos \nu_i, \sin \nu_i)^\top$  in the following way: Firstly, from  $\mathbf{t}_1 = (t_{11}, t_{12})^\top$ , we obtain  $\nu_1 = -\arccos(t_{11})$  if  $t_{12} < 0$ ;  $\nu_1 = \arccos(t_{11})$  if  $t_{12} \geq 0$ . Secondly, for  $i = 1, 2, \dots, n$  we successively compute  $\nu_{i+1}$  from  $\nu_i$ :

$$\nu_{i+1} = \begin{cases} \nu_i - \arccos(I), & \text{if } D < 0, \\ \nu_i + \arccos(I), & \text{if } D > 0, \\ \nu_i, & \text{otherwise,} \end{cases} \quad \text{where } D = \det(\mathbf{t}_i, \mathbf{t}_{i+1}), \quad I = \mathbf{t}_i \cdot \mathbf{t}_{i+1}.$$

Finally, we obtain  $\nu_0 = \nu_1 - (\nu_{n+1} - \nu_n)$ . Then the  $i$ -th unit outward normal vector  $\mathbf{n}_i$  is  $\mathbf{n}_i = (\sin \nu_i, -\cos \nu_i)^\top$ .

Let us introduce the “dual” edge  $\Gamma_i^* = [\mathbf{x}_i^*, \mathbf{x}_i] \cup [\mathbf{x}_i, \mathbf{x}_{i+1}^*]$  of  $\Gamma_i$ , where

$$\mathbf{x}_i^* = (\mathbf{x}_{i-1} + \mathbf{x}_i)/2$$

is the mid point of the  $i$ -th edge  $\Gamma_i$  ( $i = 1, 2, \dots, n$ ;  $\mathbf{x}_{n+1}^* = \mathbf{x}_1^*$ ). The length of  $\Gamma_i^*$  is  $r_i^* = (r_i + r_{i+1})/2$ .

We define the  $i$ -th tangent angle of  $\Gamma_i^*$  by

$$\nu_i^* = \frac{\nu_i + \nu_{i+1}}{2} = \nu_i + \frac{\varphi_i}{2},$$

where  $\varphi_i = \nu_{i+1} - \nu_i$  is the angle between the adjacent two edges. See Figure 3.1.

Then the  $i$ -th unit tangent vector  $\mathbf{T}_i$  and the outward unit normal vector  $\mathbf{N}_i$  at the  $i$ -th vertex  $\mathbf{x}_i$  are given by

$$\mathbf{T}_i = (\cos \nu_i^*, \sin \nu_i^*)^\top, \quad \mathbf{N}_i = (\sin \nu_i^*, -\cos \nu_i^*)^\top,$$

respectively.

### 3.3 The length $L$ , the area $A$ , and the curvatures $\{k_i\}_{i=1}^n$

The total length of  $\Gamma$  can be calculated as

$$L = \sum_{i=1}^n r_i = \sum_{i=1}^n r_i^*,$$

and the enclosed area of  $\Gamma$  can be calculated as

$$A = \frac{1}{2} \sum_{i=1}^n (\mathbf{x}_i \cdot \mathbf{n}_i) r_i = \frac{1}{2} \sum_{i=1}^n \mathbf{x}_{i-1}^\perp \cdot \mathbf{x}_i.$$

Hereafter we will use the following abbreviations:

$$c_i = \cos \frac{\varphi_i}{2}, \quad s_i = \sin \frac{\varphi_i}{2} \quad (i = 1, 2, \dots, n).$$

Then it is easy to check that

$$\begin{aligned} \mathbf{t}_i &= c_i \mathbf{T}_i + s_i \mathbf{N}_i, & \mathbf{t}_{i+1} &= c_i \mathbf{T}_i - s_i \mathbf{N}_i, \\ \mathbf{n}_i &= c_i \mathbf{N}_i - s_i \mathbf{T}_i, & \mathbf{n}_{i+1} &= c_i \mathbf{N}_i + s_i \mathbf{T}_i, \end{aligned}$$

and from which it follows that

$$\dot{L} = \sum_{i=1}^n \dot{\mathbf{x}}_i \cdot (\mathbf{t}_i - \mathbf{t}_{i+1}) = 2 \sum_{i=1}^n V_i s_i = \sum_{i=1}^n V_i k_i^* r_i^* = \sum_{i=1}^n k_i \langle v \rangle_i r_i, \quad (3.2)$$

$$\dot{A} = \sum_{i=1}^n V_i c_i r_i^* + \sum_{i=1}^n \alpha_i s_i \frac{r_{i+1} - r_i}{2} = \sum_{i=1}^n \langle v \rangle_i r_i + \text{err}_A, \quad (3.3)$$

$$\text{err}_A = \sum_{i=1}^n \langle v \rangle_i \frac{r_{i+1} - 2r_i + r_{i-1}}{4} + \sum_{i=1}^n \alpha_i s_i \frac{r_{i+1} - r_i}{2}.$$

Here  $k_i^* = 2s_i/r_i^*$  is the  $i$ -th curvature on the dual edge  $\Gamma_i^*$ ,  $\langle v \rangle_i$  is the averaged normal velocity on  $\Gamma_i$  defined as

$$\langle v \rangle_i = \frac{1}{r_i} \int_{\Gamma_i} v ds \quad (i = 1, 2, \dots, n),$$

$V_i$  is the normal velocity at  $\mathbf{x}_i$  defined as

$$V_i = \frac{\langle v \rangle_i + \langle v \rangle_{i+1}}{2c_i} \quad (i = 1, 2, \dots, n), \quad (3.4)$$

and  $k_i$  is the  $i$ -th curvature defined on  $\Gamma_i$  defined as

$$k_i = \frac{\tan(\varphi_i/2) + \tan(\varphi_{i-1}/2)}{r_i} \quad (i = 1, 2, \dots, n),$$

which is the same as the polygonal curvature in [1]. The  $i$ -th averaged normal velocity  $\langle v \rangle_i$  will be defined by (3.8) in §3.4.

The quantities  $\dot{L}$  and  $\dot{A}$  are discrete analogue of  $\dot{L} = \int_{\mathcal{C}} kV ds$  and  $\dot{A} = \int_{\mathcal{C}} V ds$  for smooth curve  $\mathcal{C}$ , if  $\text{err}_A = 0$  holds, respectively. Note that if distribution of the vertices is uniform, that is,  $r_i \equiv L/n$  holds for all  $i$ , then we have  $\text{err}_A = 0$ . Another way of realizing  $\text{err}_A = 0$  is to define  $\alpha_i = (\langle v \rangle_{i+1} - \langle v \rangle_i)/(2s_i)$ , since  $\text{err}_A = \sum_{i=1}^n (r_{i+1} - r_i)(\langle v \rangle_i - \langle v \rangle_{i+1} + 2s_i\alpha_i)/4$  holds. This way is valid for instance for the curvature flow  $\langle v \rangle_i = -k_i$  since  $\alpha_i$  does not become singular even if  $s_i = 0$ . But in general such as the Hele-Shaw flow, it is hard to compute  $\alpha_i$  near  $s_i \approx 0$ . Hence we will use the uniform distribution technique from the above reason and also from the viewpoint of numerical stability.

**Remark 3.1** Note that if we can calculate the average  $\langle \nabla p \cdot \mathbf{n}_i \rangle_i$  and put  $\langle v \rangle_i = -\langle \nabla p \cdot \mathbf{n}_i \rangle_i$ , then we have

$$\dot{A} = \sum_{i=1}^n \langle v \rangle_i r_i = - \sum_{i=1}^n \int_{\Gamma_i} \frac{\partial p}{\partial \mathbf{n}} ds = - \int_{\Gamma(t)} \frac{\partial p}{\partial \mathbf{n}} ds = - \iint_{\Omega(t)} \Delta p dx dy = 0,$$

if  $\text{err}_A = 0$ . The averaged value  $\langle \nabla p \cdot \mathbf{n}_i \rangle_i$  can not be obtained in general, but we will obtain AP-property  $\dot{A} = 0$  from another context in §3.4.

### 3.4 Step 2: Compute $\{V_i\}_{i=1}^n$ by a modified CSM (mCSM)

We compute the averaged normal velocity  $\langle v \rangle_i$  by means of a modified charge simulation method (**mCSM** in short). See §A for the original CSM under the invariant scheme and for comparison argument with the boundary element method (BEM).

For each fixed  $t \geq 0$  we solve the following Dirichlet problem:

$$\begin{cases} \Delta p = 0 & \text{in } \Omega(t), \\ p = \gamma k_i & \text{on } \Gamma_i(t) \quad (i = 1, 2, \dots, n), \end{cases}$$

by means of a CSM-type technique as follows. We seek the approximate solution  $P$  of the form

$$P(\mathbf{x}) = Q_0 + \sum_{j=1}^n Q_j E_j(\mathbf{x}), \quad E_j(\mathbf{x}) := E(\mathbf{x} - \mathbf{y}_j) - E(\mathbf{x} - \mathbf{z}), \quad (3.5)$$

where  $E$  is the fundamental solution of the Laplace operator  $\Delta$  such as

$$E(\mathbf{x}) = \frac{1}{2\pi} \log |\mathbf{x}|,$$

$\mathbf{z}$  is a “dummy” point located at a sufficiently far position ( $\mathbf{z} = (1000, 0)^T$  will be used in §4),  $\mathbf{y}_j$ 's are the charge points given by

$$\mathbf{y}_j = \mathbf{x}_j^* + d\mathbf{n}_j \quad (j = 1, 2, \dots, n),$$

and  $d > 0$  is a parameter controlling accuracy of mCSM. Note that  $P$  satisfies  $\Delta P = 0$  in  $\Omega$  and is invariant under the trivial affine transformation and the origin shift of the boundary data as well as the original invariant scheme of CSM as in §A. Thus we can add one more condition instead of (A.2) which is required for the invariance of the original invariant scheme of CSM. We select the condition such a way that the weighted average of  $Q_j$ 's is equal to 0, that is, coefficients  $\{Q_j\}_{j=0}^n$  are determined by

$$P(\mathbf{x}_i^*) = \gamma k_i \quad (i = 1, 2, \dots, n), \quad \sum_{j=1}^n Q_j H_j = 0, \quad (3.6)$$

where

$$H_j := - \sum_{i=1}^n \nabla E_j(\mathbf{x}_i^*) \cdot \mathbf{n}_i r_i \quad (j = 1, 2, \dots, n).$$

The equations (3.6) are equivalent to the system of  $n + 1$  linear equations as follows:

$$\begin{pmatrix} 0 & \mathbf{H}^T \\ \mathbf{1} & G \end{pmatrix} \begin{pmatrix} Q_0 \\ \mathbf{Q} \end{pmatrix} = \begin{pmatrix} 0 \\ \mathbf{b} \end{pmatrix}, \quad (3.7)$$

where

$$G = (E_j(\mathbf{x}_i^*)) \in \mathbb{R}^{n \times n}, \quad \mathbf{1} = (1, 1, \dots, 1)^T \in \mathbb{R}^n, \\ \mathbf{H} = (H_1, H_2, \dots, H_n)^T, \quad \mathbf{Q} = (Q_1, Q_2, \dots, Q_n)^T, \quad \mathbf{b} = (\gamma k_1, \gamma k_2, \dots, \gamma k_n)^T \in \mathbb{R}^n.$$

### AP-property

If the averaged normal velocity  $\langle v \rangle_i$ 's are defined by

$$\langle v \rangle_i = -\nabla P(\mathbf{x}_i^*) \cdot \mathbf{n}_i \quad (i = 1, 2, \dots, n), \quad (3.8)$$

then we have

$$\sum_{i=1}^n \langle v \rangle_i r_i = \sum_{j=1}^n Q_j H_j = 0. \quad (3.9)$$

This means that  $\dot{A} = 0$  holds in (3.3) if  $\text{err}_A = 0$ , that is, AP-property holds in a discrete sense. By using these  $\langle v \rangle_i$ 's, we define the normal velocity  $V_i$  at the  $i$ -th vertex  $\mathbf{x}_i$  by (3.4).

### Asymptotic CS-property

From (3.2) and (3.6), for the averaged normal velocity (3.8) we have

$$\begin{aligned} \dot{L} &= \sum_{i=1}^n k_i \langle v \rangle_i r_i = - \sum_{i=1}^n k_i \nabla P(\mathbf{x}_i^*) \cdot \mathbf{n}_i r_i = - \frac{1}{\gamma} \sum_{i=1}^n P(\mathbf{x}_i^*) \nabla P(\mathbf{x}_i^*) \cdot \mathbf{n}_i r_i \\ &= - \frac{1}{\gamma} \sum_{i=1}^n \int_{\Gamma} P(\mathbf{x}_i^*) \nabla P(\mathbf{x}_i^*) \cdot \mathbf{n}_i ds \\ &\approx - \frac{1}{\gamma} \sum_{i=1}^n \int_{\Gamma_i} P(\mathbf{x}) \nabla P(\mathbf{x}) \cdot \mathbf{n}_i ds \\ &= - \frac{1}{\gamma} \int_{\Gamma} P(\mathbf{x}) \nabla P(\mathbf{x}) \cdot \mathbf{n} ds \\ &= - \frac{1}{\gamma} \iint_{\Omega} \text{div}(P \nabla P) dx dy = - \frac{1}{\gamma} \iint_{\Omega} |\nabla P|^2 dx dy \leq 0. \end{aligned}$$

The above approximation “ $\approx$ ” is the equality “=” with an error of order  $1/n$  as  $n \rightarrow \infty$ . We will see this fact as follows. Put  $f_i(\mathbf{x}) = P(\mathbf{x}) \nabla P(\mathbf{x}) \cdot \mathbf{n}_i$  for  $\mathbf{x} \in \Gamma_i$ . Then by the mean value theorem, there exists  $\mu_i \in (0, 1)$  for each  $i$  such that the following estimate holds.

$$\begin{aligned} \dot{L} + \frac{1}{\gamma} \iint_{\Omega} |\nabla P|^2 dx dy &\leq \left| \frac{1}{\gamma} \iint_{\Omega} |\nabla P|^2 dx dy + \dot{L} \right| \\ &= \left| \frac{1}{\gamma} \sum_{i=1}^n \int_{\Gamma_i} (P(\mathbf{x}) \nabla P(\mathbf{x}) - P(\mathbf{x}_i^*) \nabla P(\mathbf{x}_i^*)) \cdot \mathbf{n}_i ds \right| \\ &= \left| \frac{1}{\gamma} \sum_{i=1}^n \int_{\Gamma_i} (f_i(\mathbf{x}) - f_i(\mathbf{x}_i^*)) ds \right| \\ &= \left| \frac{1}{\gamma} \sum_{i=1}^n \int_{\Gamma_i} \nabla f_i((1 - \mu_i)\mathbf{x} + \mu_i \mathbf{x}_i^*) \cdot (\mathbf{x} - \mathbf{x}_i^*) ds \right| \\ &\leq \frac{1}{\gamma} \sum_{i=1}^n C_i \max_{\mathbf{x} \in \Gamma_i} |\mathbf{x} - \mathbf{x}_i^*| r_i \leq \frac{C}{\gamma} \sum_{i=1}^n r_i^2 \leq \frac{C}{\gamma} L r_{\max}, \end{aligned}$$

where

$$C_i = \max_{\mathbf{x} \in \Gamma_i} |\nabla f_i(\mathbf{x})|, \quad C = \max_{1 \leq i \leq n} C_i, \quad r_{\max} = \max_{1 \leq i \leq n} r_i.$$

By the asymptotic uniform distribution method (3.10) below, we have

$$r_{\max} \leq \frac{L(t)}{n} + e^{-f(n,t)}$$

where  $f(n, t)$  is a given function diverging to infinity as  $t$  tends to the final time  $T \leq \infty$  or  $n \rightarrow \infty$ . In our experiment, we take  $\partial_t f(n, t) = \omega$  with  $\omega = 10n$  in §4.

Thus we have the following asymptotic CS-property:

$$\dot{L} \leq -\frac{1}{\gamma} \iint_{\Omega} |\nabla P|^2 dx dy + \frac{C}{\gamma} L \left( \frac{L}{n} + e^{-f(n,t)} \right).$$

**Remark 3.2 (BEM)** By means of the boundary element method (BEM) with the constant element, the averaged normal velocity  $\langle v \rangle_i$  can be computed from the following linear equations:

$$\frac{1}{2} \gamma_i = \sum_{j=1}^n \int_{\Gamma_j} E(\mathbf{x} - \mathbf{x}_i^*) q_j ds - \sum_{j=1}^n \int_{\Gamma_j} b_j \frac{\partial E}{\partial \mathbf{n}}(\mathbf{x} - \mathbf{x}_i^*) ds \quad (i = 1, 2, \dots, n),$$

which are derived from (A.5) in the case where  $\mathcal{C} = \Gamma$ ,  $\boldsymbol{\xi} = \mathbf{x}_i^*$ , and  $\tilde{P}$  satisfies

$$\tilde{P}(\mathbf{x}) \equiv \gamma k_i =: b_i, \quad \frac{\partial \tilde{P}}{\partial \mathbf{n}}(\mathbf{x}) \equiv q_i$$

for all  $\mathbf{x} \in \Gamma_i$ . Therefore if we define matrices  $G = (G_{ij}) \in \mathbb{R}^{n \times n}$  and  $H = (H_{ij}) \in \mathbb{R}^{n \times n}$  by

$$G_{ij} = \int_{\Gamma_j} E(\mathbf{x} - \mathbf{x}_i^*) ds, \quad H_{ij} = \frac{1}{2} \delta_{ij} + \int_{\Gamma_j} \frac{\partial E}{\partial \mathbf{n}}(\mathbf{x} - \mathbf{x}_i^*) ds,$$

respectively, then the above relations are equivalent to the following simultaneous equations:

$$G\mathbf{q} = H\mathbf{b},$$

where  $\mathbf{q} = (q_1, q_2, \dots, q_n)^T$ ,  $\mathbf{b} = (b_1, b_2, \dots, b_n)^T \in \mathbb{R}^n$ . Solving the above simultaneous equations for  $\mathbf{q}$ , we obtain the averaged normal velocity such as

$$\langle v \rangle_i = -q_i \quad (i = 1, 2, \dots, n).$$

We note that  $G_{ij}$  and  $H_{ij}$  can be calculated analytically. However, it is unclear whether CS-property and AP-property hold or not.

### 3.5 Step 3: Compute $\{\alpha_i\}_{i=1}^n$ by the asymptotic uniform distribution method (UDM)

To realize uniform distribution asymptotically (c.f. [12]), we assume that

$$r_i - \frac{L}{n} = \eta_i e^{-f(n,t)}, \quad (3.10)$$

where  $f$  is a given function satisfying

$$f(n,t) \rightarrow \infty \quad \text{as } t \rightarrow T \leq \infty \text{ or } n \rightarrow \infty$$

with the final time  $T$  of the problem, and

$$\sum_{i=1}^n \eta_i = 0, \quad |\eta_i| \leq 1 \quad (i = 1, 2, \dots, n).$$

By using a relaxation term  $\omega(n,t) = \partial_t f(n,t)$  we obtain

$$\dot{r}_i - \frac{\dot{L}}{n} = \left( \frac{L}{n} - r_i \right) \omega(n,t) \quad (i = 1, 2, \dots, n), \quad \int_0^T \omega(n,t) dt = \infty.$$

In our experiment,  $\omega(n,t)$  is taken such as a constant  $\omega = 10n$  in §4.

Taking into account the relations

$$\dot{r}_i = (\dot{\mathbf{x}}_i - \dot{\mathbf{x}}_{i-1}) \cdot \mathbf{t}_i = V_i s_i + V_{i-1} s_{i-1} + c_i \alpha_i - c_{i-1} \alpha_{i-1} = \frac{\dot{L}}{n} + \left( \frac{L}{n} - r_i \right) \omega(n,t),$$

we deduce  $n - 1$  equations for tangential velocities  $\alpha_i$  ( $i = 2, 3, \dots, n$ ):

$$\alpha_i = \frac{\Psi_i}{c_i} + \frac{c_1}{c_i} \alpha_1,$$

$$\Psi_i = \psi_2 + \psi_3 + \dots + \psi_i,$$

$$\psi_i = -V_i s_i - V_{i-1} s_{i-1} + \frac{\dot{L}}{n} + \left( \frac{L}{n} - r_i \right) \omega(n,t).$$

To determine  $\alpha_1$ , we add one more linear equation of the form  $\sum_{i=1}^n \alpha_i b_i = B$ , which is independent of the above  $n - 1$ . If we put

$$C = \sum_{i=2}^n \frac{b_i}{c_i} \Psi_i, \quad D = c_1 \sum_{i=1}^n \frac{b_i}{c_i}, \quad (3.11)$$

we obtain  $\alpha_1 = (B - C)/D$ . Next, we propose two candidates for each  $\{b_i\}_{i=1}^n$  and  $B$ , and choose one of them in the following way:

### Candidate 1

We put

$$b_i = s_i \frac{r_{i+1} - r_i}{2} \quad (i = 1, 2, \dots, n), \quad B = - \sum_{i=1}^n \langle v \rangle_i \frac{r_{i+1} - 2r_i + r_{i-1}}{4},$$

and from (3.11) we calculate  $C$  and  $D$ . We denote this  $D$  by  $D_1$ . If the above equation holds, then  $\text{err}_A = 0$  and  $\dot{A} = \sum_{i=1}^n \langle v \rangle_i r_i$  hold in (3.3). However, if distribution of grid points is almost uniform, then the above equation is almost nothing. Therefore we need another candidate.

### Candidate 2

The second candidate of a linear equation is the zero-average condition  $\sum_{i=1}^n \alpha_i r_i^* = 0$ , that is,  $b_i = r_i^*$  for  $i = 1, 2, \dots, n$  and  $B = 0$  (see [12] in detail). From this and (3.11) we calculate  $C$  and  $D$ . We denote this  $D$  by  $D_2$ .

### Choice one from two candidates

For calculating  $\alpha_1$  we use Candidate 1, if  $|D_1| > |D_2|$ , and Candidate 2, otherwise.

## 4 Numerical experiments

The parameters have been chosen as follows:

- $n = 100$  (the number of grid points);
- $\gamma = 1$  (the surface tension coefficient);
- $\mathbf{z} = (1000, 0)^T$  (the “dummy” point in mCSM approximation (3.5));
- $\tau = 1/(10n^2)$  (the time-mesh size);
- $\omega = 10n$  (the relaxation term);
- $d = n^{-1/2}$  (the parameter controlling accuracy of mCSM).

The initial curve  $\Gamma : [0, 1] \ni u \mapsto (x_1(u), x_2(u))^T \in \mathbb{R}^2$  is given by

$$x_1(u) = \cos z(u), \quad x_2(u) = 0.7 \sin z(u) + \sin x_1(u) + x_3(u)^2,$$

where  $z = 2\pi u$ ,  $x_3(u) = \sin(3z(u))$  for  $u \in [0, 1]$ . See Figure 4.1 (a). Let us examine the results of our numerical computation in order.

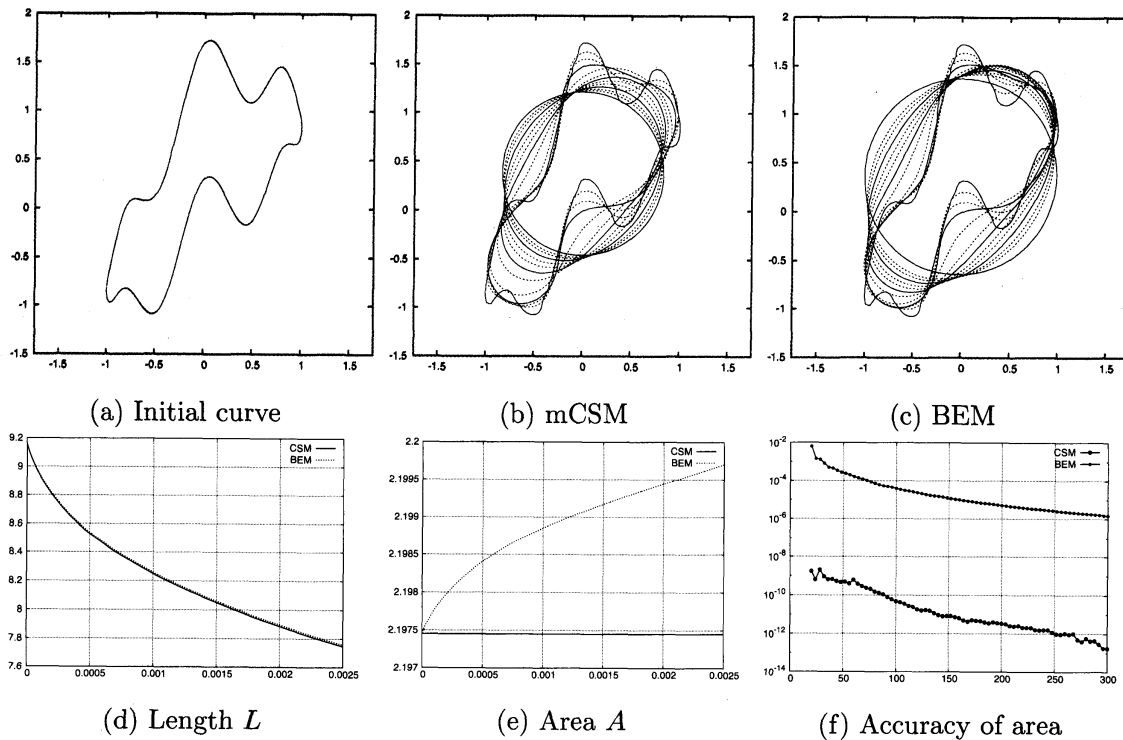


Figure 4.1: Results of numerical computation: (a) the initial curve; time evolution of boundary curves (b) mCSM; (c) BEM; (d) time evolution of length; (e) time evolution of area; (f) the accuracy of area

- Time evolutions of boundary curves are indicated in Figure 4.1 (b) and (c), when the normal velocity is computed by mCSM and BEM, respectively. Although in both cases the boundary curves converge to circles, their size seem to be different.
- Figure 4.1 (d) shows the time evolution of the length  $L(t)$  of the boundary curve, where the horizontal axis and the vertical axis represent the time  $t$  and the length  $L$ , respectively. It can be observed that the length decreases monotonically for both methods: mCSM and BEM. As we have seen in §3.4, when the normal velocity is computed by mCSM, we can prove that  $\dot{L}$  takes a negative value plus a small error for a large  $n$  or  $t$ , since the approximate solution by mCSM is smooth in a neighborhood of  $\bar{\Omega}$ . On the other hand, when the normal velocity is computed by BEM, there exist singularities on the boundary curve  $\Gamma$ , therefore we can not use a useful mathematical tool such as the divergence theorem, and this makes it difficult to analyze the evolution of the length. However, CS-property is observed numerically.
- Figure 4.1 (e) shows the time evolution of the enclosed area  $A(t)$  of the boundary curve, where the horizontal axis and the vertical axis represent the time  $t$  and

the area  $A$ , respectively. Concerning the time evolution of the area, there is a big difference. In both methods of mCSM and BEM, the tangential velocity is computed by UDM, therefore  $\text{err}_A$  converges to 0 exponentially as  $t \rightarrow T$  or  $n \rightarrow \infty$ . When we compute the normal velocity by mCSM, AP-property is achieved in maximal accuracy in double-precision arithmetic. On the other hand, when the normal velocity is computed by BEM, AP-property does not hold. Indeed, the area increases in time. We can guess that this is a reason why the size of limiting circles are different.

- Figure 4.1 (f) shows the accuracy of area, where the horizontal axis and the vertical axis represent the number of grid points  $n$  and the error  $\text{err}(n)$ , respectively. The error is measured by

$$\text{err}(n) = \max_{1 \leq j \leq M} \left| \frac{A^j(n) - A^0(n)}{A^0(n)} \right|,$$

where

- $n$  is the number of grid points, which is taken such as  $n = 4k$  ( $k = 5, 6, \dots, 75$ );
- $A^0(n)$  denotes the enclosed area of the initial  $n$ -sided closed polygonal plane curve;
- $A^j(n)$  denotes the enclosed area of the boundary curve with  $n$  vertices at the  $j$ -th step;
- $M$  denotes the calculation frequency, and it is chosen as  $M = 1000$  here.

It can be observed that there are differences of accuracy about 6–7 digits between in two methods, and this implies that our proposal scheme computing the normal velocity by mCSM is much better than that by BEM.

## 5 Conclusion

In the present paper, a modified charge simulation method combined with the asymptotic uniform distribution method was proposed for an approximation scheme of the one-phase interior Hele-Shaw problem. The methods satisfy the asymptotic curve-shortening property and the area-preserving property, while the boundary element method does not satisfy area-preserving property.

Our methods can be applied for Hele-Shaw problems in several situations including one-phase exterior Hele-Shaw problem, one-phase Hele-Shaw problem with sink or source, and so on. These results will be reported in the forthcoming paper.

## A The original invariant scheme of CSM

We explain the invariant scheme of the charge simulation method (CSM) [9, 10] briefly. Let  $\mathcal{D}$  be a bounded region in  $\mathbb{R}^2$  with a smooth boundary  $\mathcal{C} = \partial\mathcal{D}$ . We consider the following potential problem:

$$\begin{cases} \Delta p = 0 & \text{in } \mathcal{D}, \\ p = f & \text{on } \mathcal{C}, \end{cases} \quad (\text{A.1})$$

where  $f$  is a given function defined on  $\mathcal{C}$ . The invariant scheme of CSM gives an approximate solution  $P$  as in the following three steps:

- (1) Put  $n$  points  $\{\mathbf{y}_j\}_{j=1}^n$  in  $\mathbb{R}^2 \setminus \overline{\mathcal{D}}$ .
- (2) Construct the approximate solution  $P$  as follows:

$$P(\mathbf{x}) = Q_0 + \sum_{j=1}^n Q_j E(\mathbf{x} - \mathbf{y}_j), \quad E(\mathbf{x}) = \frac{1}{2\pi} \log |\mathbf{x}|$$

with the constraint

$$\sum_{j=1}^n Q_j = 0. \quad (\text{A.2})$$

- (3) Determine coefficients  $\{Q_j\}_{j=0}^n$  by the collocation method: Put  $n$  points  $\{\mathbf{x}_i\}_{i=1}^n$  on the boundary  $\mathcal{C}$ , and impose the conditions

$$P(\mathbf{x}_i) = f(\mathbf{x}_i) \quad (i = 1, 2, \dots, n). \quad (\text{A.3})$$

The above procedure is typical algorithm of the invariant scheme of CSM. We note that  $P$  satisfies the Laplace equation exactly in  $\mathcal{D}$ . Furthermore, the conditional expressions (A.2) and (A.3) are equivalent to the system of  $n + 1$  linear equations as follows:

$$\begin{pmatrix} 0 & \mathbf{1}^T \\ \mathbf{1} & G \end{pmatrix} \begin{pmatrix} Q_0 \\ \mathbf{Q} \end{pmatrix} = \begin{pmatrix} 0 \\ \mathbf{f} \end{pmatrix}, \quad (\text{A.4})$$

where

$$G = (E(\mathbf{x}_i - \mathbf{y}_j)) \in \mathbb{R}^{n \times n}, \quad \mathbf{1} = (1, 1, \dots, 1)^T \in \mathbb{R}^n, \\ \mathbf{Q} = (Q_1, Q_2, \dots, Q_n)^T, \quad \mathbf{f} = (f(\mathbf{x}_1), f(\mathbf{x}_2), \dots, f(\mathbf{x}_n))^T \in \mathbb{R}^n.$$

CSM is a very simple numerical scheme for potential problems since we do not need to perform mesh division in  $\mathcal{D}$  such as the finite element method, but only choose points outside and on the boundary of  $\mathcal{D}$ . Nevertheless, under some conditions, the error of the

approximate solution decays exponentially with respect to  $n$ . Owing to this impactful property, the computational cost is low. Moreover, coding the program is very easy, since we only have to solve the linear equation (A.4). We note that  $P$  is invariant under the trivial affine transformation

$$\mathbf{x} \rightarrow s\mathbf{x}, \quad \mathbf{y}_j \rightarrow s\mathbf{y}_j,$$

where  $s \neq 0$  is a real constant, and the origin shift of the boundary data

$$f(\mathbf{x}) \rightarrow f(\mathbf{x}) + \mathbf{c},$$

where  $\mathbf{c} \in \mathbb{R}^2$ .

Since CSM's approximate solution is sufficiently smooth in a neighborhood of  $\overline{\mathcal{D}}$ , if we approximate the pressure and compute the normal velocity by CSM, then CS-property holds approximately. However, AP-property does not hold in general, since  $\sum_{i=1}^n \langle v \rangle_i r_i = 0$  is not assured even if  $\text{err}_A = 0$ . Therefore we have used a modified invariant scheme of CSM in order to satisfy  $\sum_{i=1}^n \langle v \rangle_i r_i = 0$  in (3.9).

### Comparison argument with the boundary element method (BEM)

In order to solve (A.1) by the boundary element method (BEM) which is popular for solving partial differential equations, we have to derive some integral equation as follows:

$$\frac{\theta(\boldsymbol{\xi})}{2\pi} \tilde{P}(\boldsymbol{\xi}) = \int_{\mathcal{C}} E(\mathbf{x} - \boldsymbol{\xi}) \frac{\partial \tilde{P}}{\partial \mathbf{n}}(\mathbf{x}) ds - \int_{\mathcal{C}} f(\mathbf{x}) \frac{\partial E(\mathbf{x} - \boldsymbol{\xi})}{\partial \mathbf{n}} ds \quad (\boldsymbol{\xi} \in \mathcal{C}), \quad (\text{A.5})$$

where  $\tilde{P}$  is an approximate solution of (A.1) and  $\theta(\boldsymbol{\xi})$  is a function defined by

$$\theta(\boldsymbol{\xi}) = \begin{cases} \text{inner angle at } \boldsymbol{\xi} & \text{if } \boldsymbol{\xi} \text{ is a corner,} \\ \pi & \text{if } \boldsymbol{\xi} \text{ is a smooth point.} \end{cases}$$

In general, we divide  $\mathcal{C}$  into finite line segments which are called boundary elements, and the above integral equation is represented as a finite sum of integrals on each boundary element, that is, the boundary  $\mathcal{C}$  is approximated by a polygon.

## References

- [1] M. Beneš, M. Kimura and S. Yazaki, *Second order numerical scheme for motion of polygonal curves with constant area speed*, Interfaces Free Bound. **11** (2009) 515–536.
- [2] C. L. Epstein and M. Gage, *The curve shortening flow*, Math. Sci. Res. Inst. Publ. **7** (1987) 15–59.

- [3] B. Gustafsson and A. Vasil'ev, *Conformal and Potential Analysis in Hele-Shaw Cells*, Birkhaeuser (2006).
- [4] H. S. Hele-Shaw, *The flow of water*, Nature **58** (1898) 34–36, 520.
- [5] M. Katsurada and H. Okamoto, *A mathematical study of the charge simulation method. I*, J. Fac. Sci. Univ. Tokyo Sect. IA Math. **35** (1988) 507–518.
- [6] M. Kimura, *Numerical analysis for moving boundary problems using the boundary tracking method*, Japan J. Ind. Appl. Math. **14** (1997) 373–398.
- [7] M. Kimura and H. Notsu, *A level set method using the signed distance function*, Japan J. Indust. Appl. Math. **19** (2002) 415–446.
- [8] H. Lamb, *Hydrodynamics*, 6th edition, Dover Publications (1945).
- [9] K. Murota, *On “invariance” of schemes in the fundamental solution method* (Japanese), Information Processing Society of Japan **43** (1993) 533–535.
- [10] K. Murota, *Comparison of conventional and “invariant” schemes of fundamental solutions method for annular domains*, Japan J. Indust. Appl. Math. **12** (1995) 61–85.
- [11] H. Okamoto and M. Katsurada, *A rapid solver for the potential problems* (Japanese), The Japan Society for Industrial and Applied Mathematics **2** (1992) 212–230.
- [12] D. Ševčovič and S. Yazaki, *On a gradient flow of plane curves minimizing the anisoperimetric ratio*, IAENG International Journal of Applied Mathematics **43** (2013) 160–171.
- [13] M. J. Shelley, F.-R. Tian and K. Wlodarski, *Hele-Shaw flow and pattern formation in a time-dependent gap*, Nonlinearity **10** (1997) 1471–1495.
- [14] M. Shōji, *An application of the charge simulation method to a free boundary problem*, J. Fac. Sci. Univ. Tokyo Sect. IA Math. **33** (1986) 523–539.
- [15] S. Yazaki, *A numerical scheme for the Hele-Shaw flow with a time-dependent gap by a curvature adjusted method*, Advanced Studies in Pure Mathematics **64** (2014) 253–261.